Available online at www.sciencedirect.com

SCIENCE DIRECT®

Journal of Catalysis 239 (2006) 117–124

JOURNAL OF CATALYSIS

www.elsevier.com/locate/jcat

Effect of hydrogen addition on SO_2 tolerance of silver–alumina for SCR of NO with propane

Ken-ichi Shimizu *, Takaaki Higashimata, Masao Tsuzuki, Atsushi Satsuma

Department of Applied Chemistry, Graduate School of Engineering, Nagoya University, Chikusa-ku, Nagoya 464-8603, Japan

Received 27 October 2005; revised 6 January 2006; accepted 9 January 2006

Abstract

The effect of H_2 addition and silver loading on the SO_2 tolerance and de-NO_x performance of Ag/Al_2O_3 for the C_3H_8-SCR reaction was investigated by catalytic testing combined with various characterization results. SO_2 tolerance is improved by H_2 cofeeding as well as an increase in Ag loading of Ag/Al_2O_3. In situ IR results shows that the reaction of sulfates on Ag-containing sites with H_2 results in the desorption of SO_2 or migration of the sulfates to alumina surface. TPD/TRP results show that sulfate desorption in He or in H_2 occurs at lower temperature for the higher loading sample. Combined with UV–vis and in situ IR results, these findings suggest that the higher SO_2 tolerance of high loading catalyst for the H_2–C_3H_8-SCR reaction is caused by the higher rate of sulfate reduction that is more advantageous over partially reduced silver sites than over Ag^+ sites.

Keywords: Nitrogen oxides; Silver alumina; Reduction; Sulfur oxide

1. Introduction

The selective catalytic reduction of NO by hydrocarbons (HC-SCR) in the presence of excess oxygen is a potential method of removing NO_x from lean-burn and diesel exhausts [1–4]. Ag/Al_2O_3 is among the most active catalysts for SCR by alcohol [5–7] or higher hydrocarbons [8–11] under lean-burn exhaust conditions and shows moderate tolerance to SO_2 [7,8, 12–17]. Recently, much attention has focused on the “hydrogen effect” on the SCR performance of Ag/Al_2O_3. The first report by Satokawa [18] and our research group [19] and subsequent studies [20–24] demonstrated that Ag/Al_2O_3 shows significantly higher activity in the presence of hydrogen (H_2-HC-SCR condition) than in the absence of it (HC-SCR condition). Because of the high activity under high GHSV conditions as well as at relatively low reaction temperatures, this catalytic system could be a promising candidate for practical use if the catalyst has high SO_2 tolerance. Satokawa and our research group [19] showed that 2 wt% Ag/Al_2O_3 exhibited high SO_2 tolerance in the low SO_2 concentration condition; the NO conversion did not decrease in the presence of 6.4 ppm SO_2 and 9.1% H_2O at 723 K for 9 h.

Several authors have studied the SO_2-poisoning mechanism and the factors affecting SO_2 resistance of the Ag/Al_2O_3 catalysts for HC-SCR in the absence of hydrogen [7,12–17]. It was reported that the degree of deactivation depends on the silver loading [16,17], reaction temperature [12], and type of reductant used (alkane or alkene) [16]. Although many studies have revealed that around 2 wt% Ag is an optimum loading on alumina for HC-SCR in the absence of SO_2, Park et al. [17] and Angelidis et al. [16] showed that higher loading Ag/Al_2O_3 catalyst shows higher NO reduction activity in the presence of SO_2. Meunier and Ross [14] studied the effect of SO_2 on C_3H_6-SCR activity of 1.2 wt% Ag/Al_2O_3 and found that the addition of 100 ppm SO_2 results in a significant drop in NO and propene conversions, possibly caused by the sulfation of the silver species. Considering the highly attractive nature of H_2-HC-SCR reaction over Ag/Al_2O_3, the fundamental information on the SO_2 poisoning and SO_2 tolerance in H_2-HC-SCR should be clarified. In this study we show the effect of H_2 addition on the SO_2 tolerance and de-NO_x performance of Ag/Al_2O_3 with various silver loadings. In situ IR and UV–vis

---

* Corresponding author. Fax: +81 52 789 3193.
E-mail address: kshimizu@apchem.nagoya-u.ac.jp (K. Shimizu).

0021-9517/$ – see front matter © 2006 Elsevier Inc. All rights reserved.
doi:10.1016/j.jcat.2006.01.011

spectroscopic experiments and TPD/TPR were performed to characterize the structure surface sulfates and Ag species and to investigate the effect of H_2 addition and silver loading on SO_2 tolerance.

2. Experimental

The Ag/Al_2O_3 catalyst (Ag = 2, 3, 4, 5 wt%) was prepared by impregnating γ-AlOOH with an aqueous solution of silver nitrate, followed by evaporation to dryness at 393 K and then calcination in air at 873 K for 4 h. The catalytic test was performed in a fixed-bed flow reactor at a flow rate of 100 $cm^3\,min^{-1}$. Typical compositions of feed gas in the absence and presence of H_2 were $NO/C_3H_8/O_2/He = 0.1\%/0.1\%/10\%/\text{balance}$ and $NO/C_3H_8/O_2/H_2/He = 0.1\%/0.1\%/10\%/0.5\%/\text{balance}$, respectively. The effluent gases, including N_2, CO_x ($CO + CO_2$) and NO_x ($NO + NO_2$), were analyzed by GC and NO_x analysis (Best BCL-100uH).

Temperature-programmed desorption (TPD) in a flow of He flow (60 $cm^3\,min^{-1}$) and temperature-programmed reaction (TPR) in a flow of $H_2(0.5\%)/He$ (60 $cm^3\,min^{-1}$) were carried out using TPD equipment (BEL JAPAN). The sulfated Ag/Al_2O_3 catalysts (0.2 g) were first prepared by exposing them to a flow of $SO_2(50\ ppm)/H_2O(3\%)/O_2(10\%)/H_2(0.5\%)/NO(0.1\%)/C_3H_8(0.1\%)$ at flow rate of 100 $cm^3\,min^{-1}$ (GHSV = 19,000 h^{-1}) for 7 h at 623 K. The sulfated sample (0.02 g) was transferred to the TPD cell and purged with He at 323 for 0.5 h. Then TPD or TPR was performed at a reduced pressure (200 Torr) from 323 to 1073 K at a heating rate of 10 $K\,min^{-1}$, and outlet gases were analyzed by mass spectrometry. The quantification of SO_2 ($m/e = 64$) was carried out by calibration of the mass response using the SO_2(50 ppm)/He mixture.

In situ IR spectra were recorded on a JASCO FT/IR-620 equipped with a quartz IR cell connected to a conventional flow reaction system, as was used in our previous study [20]. The sample was pressed into a 0.04 g of self-supporting wafer and mounted into the quartz IR cell with CaF_2 windows. The spectra were measured accumulating 30–100 scans at a resolution of 2 cm^{-1}. A reference spectrum of the catalyst wafer in He taken at measurement temperature was subtracted from each spectrum. Before each experiment, the catalyst disk was heated in 10% O_2/He at 773 K for 1 h, followed by cooling to the desired temperature and purging for 30 min in He. Then a flow of various gas mixtures was fed at a rate of 100 $cm^3\,min^{-1}$. Typical compositions of feed gas were the same as those in the reaction experiments. The time-resolved change in the outlet concentration of reactants or products was monitored by quadrupole mass spectrometry. To prevent changes in the operating pressure of IR cell, the excess flow from the cell was vented.

The diffuse reflectance UV–vis spectra of catalysts were measured with a JASCO V-570. The sample (0.2 g) was exposed to various gas mixtures at 623 K and quenched at room temperature. Then UV–vis spectra of the quenched sample were measured after moving into an optical quartz cell without exposure to the air.

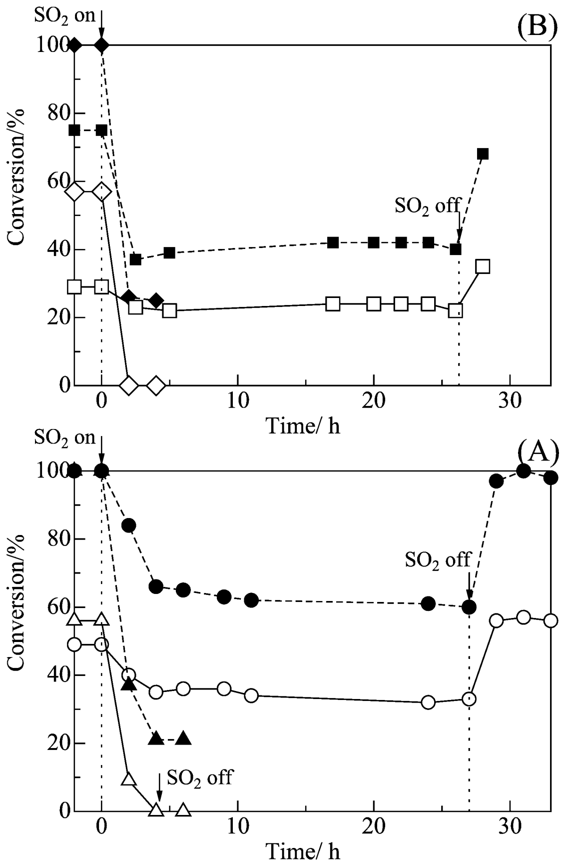

Fig. 1. The effect of SO_2 addition on NO conversion to N_2 (open symbols) and C_3H_8 conversion to CO_x (closed symbols) for SCR at 773 K; (A) 3 wt% Ag/Al_2O_3 in the absence (△, ▲) or in the presence 0.5% H_2 (○, ●), (B) (◇, ◆) 2 wt% Ag/Al_2O_3 and (□, ■) 4 wt% Ag/Al_2O_3 in the presence 0.5% H_2. Conditions: 0.1% NO, 0.1% C_3H_8, 0% or 0.5% H_2, 10% O_2, 3% H_2O, 50 ppm SO_2, SV = 190,000 h^{-1}.

3. Results and discussion

3.1. Effect of SO_2 on de-NO_x performance of Ag/Al_2O_3

Fig. 1A shows the effect of SO_2 addition on the catalytic activity of 3 wt% Ag/Al_2O_3 at 773 K. After the measurement of steady-state conversions in SO_2 free condition ($t = 0$ h), 50 ppm SO_2 was added to the reaction gas mixture, and NO and C_3H_8 conversions were measured as a function of time. In the absence of H_2, the NO and C_3H_8 conversions sharply decreased when 50 ppm SO_2 was added to the reaction gas mixture, and the catalyst was completely deactivated after 4 h. Removing SO_2 from the mixture did not recover the conversions. In the presence of H_2, conversion decreased after SO_2 addition, and stable conversions were obtained after 4 h. Removing SO_2 from the gas stream fully recovered the conversions. These results suggest that H_2 addition effectively inhibits catalyst deactivation by SO_2 and also removes SO_x adspecies that poison the active site.

Ag/Al_2O_3 catalysts with different silver loadings (2 and 4 wt%) were also tested for SO_2 tolerance in H_2–C_3H_8-SCR conditions (Fig. 1B). The NO conversion for the high loading sample (4 wt%) decreased slightly on exposure to SO_2 (from

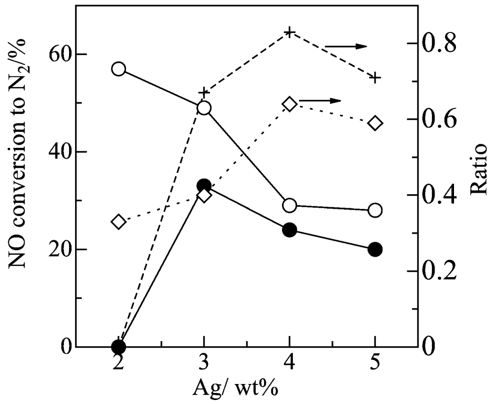

Fig. 2. Effect of silver loading on the NO conversion (○) in the absence or (●) in the presence of 50 ppm SO_2 and (+) SO_2-tolerance factor H_2–C_3H_8-SCR at 773 K. The ratio of IR band intensity due to Ag–SO_4^{2-} (1270 cm^{-1}) to that due to Al–SO_4^{2-} (1350 cm^{-1}) (from Fig. 5) is also plotted (◇).

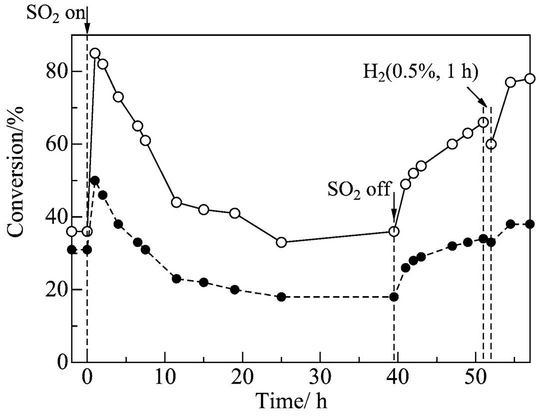

Fig. 3. The effect of SO_2 addition on NO conversion to N_2 (○) and C_3H_8 conversion to CO_x (●) for H_2–C_3H_8-SCR by 4 wt% Ag/Al_2O_3 at 623 K. Conditions: 0.1% NO, 0.2% C_3H_8, 0.5% H_2, 10% O_2, 3% H_2O, 50 ppm SO_2, SV = 19,000 h^{-1}.

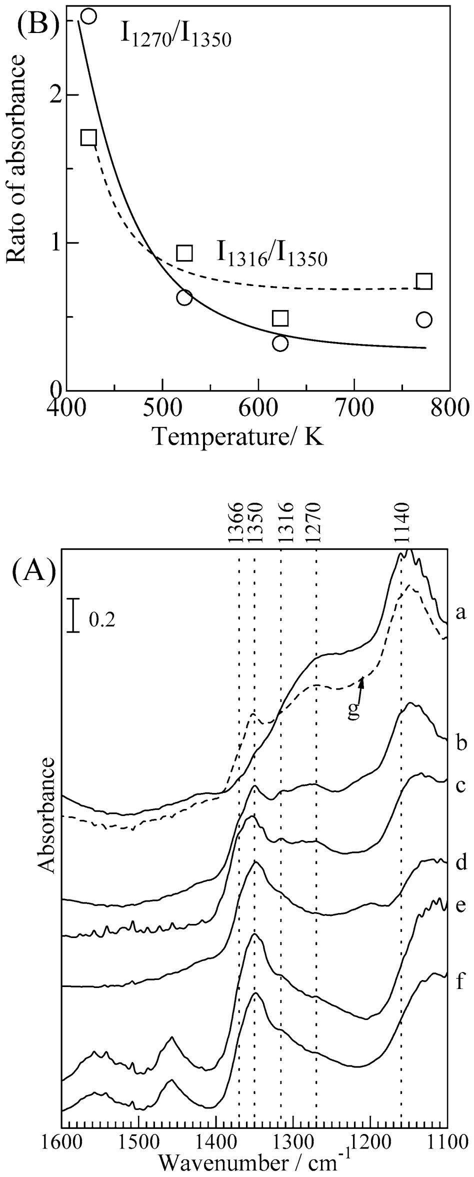

Fig. 4. (A) IR spectra of adsorbed species on 4 wt% Ag/Al_2O_3 in a flow of $SO_2/H_2O/O_2/H_2$ at (a) 423, (b) 523, (c) 623, and (d) 773 K after 2 h, (e) in a flow of $SO_2/H_2O/O_2/NO/C_3H_8$ at 773 K for 3 h, and (f) in a flow of $SO_2/H_2O/O_2/H_2/NO/C_3H_8$ at 773 K for 2 h. Spectrum g is taken by purging in He for 0.5 h at 423 K after the measurement of the spectrum a. (B) Temperature dependence of IR band intensity ratio estimated from the results in Fig. 4A.

29 to 24%), and the conversions were recovered when SO_2 was removed from the gas stream. In contrast, NO conversion for the low loading sample (2 wt%) decreased from 57 to 0% after 2 h of SO_2 cofeeding, and the catalyst was completely deactivated even when SO_2 was removed from the gas stream (results not shown). The steady-state NO conversion before and after SO_2 addition is plotted in Fig. 2 as a function of silver loading. Although NO conversion in the absence of SO_2 was higher for the lower loading catalyst, the highest activity in the presence of SO_2 was achieved on the medium-loading sample (3 wt%). The degree of SO_2 tolerance is evaluated by the ratio of NO conversion in the presence of SO_2 to that in absence of SO_2 (SO_2 tolerance factor) and plotted as a function of silver loading in Fig. 2. The SO_2 tolerance factor was highest for the 4 wt% Ag/Al_2O_3.

The 4 wt% Ag/Al_2O_3 catalyst exhibited high SO_2 tolerance at lower temperatures (623 K), as shown in Fig. 3. The NO and C_3H_8 conversions sharply increased after SO_2 addition in the H_2–C_3H_8-SCR reaction gas mixture, and maximum NO conversion (85%) was obtained. Then the conversions decreased and leveled off at 33–36%, which is close to the values before SO_2 addition. When SO_2 was removed from the gas stream, the conversions increased from 36 to 66% for 11 h. Then the flowing gas was switched to 0.5% H_2. After the hydrogen treatment for 1 h at 623 K, the NO conversion in the H_2–C_3H_8-SCR reaction reached 78% after 5 h, which is close to the initial conversion in the presence of SO_2. These results suggest that the poisoning SO_x adspecies are removed form the catalyst surface by a flow of H_2-containing mixtures.

3.2. *Sulfate formation on Ag/Al_2O_3*

Fig. 4A, spectra a–d shows IR spectra of adsorbed species on 4 wt% Ag/Al_2O_3 after 2 h of exposure of a $SO_2/H_2O/O_2/H_2$ mixture at various temperatures (423–773 K). Bands at 1366,

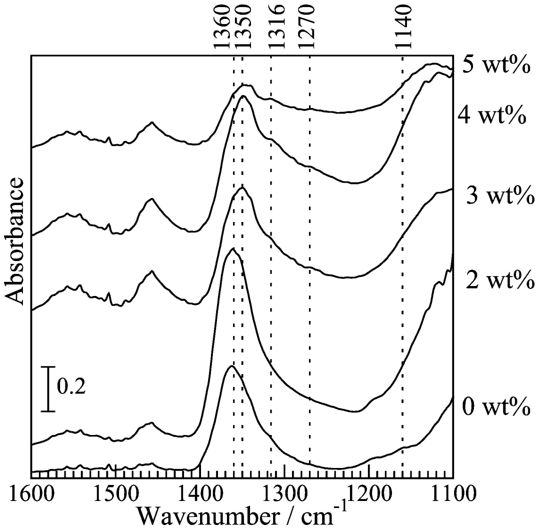

Fig. 5. IR spectra of adsorbed species on Ag/Al_2O_3 with various silver loadings in a flow of $SO_2/H_2O/O_2/H_2/NO/C_3H_8$ at 773 K for 2 h.

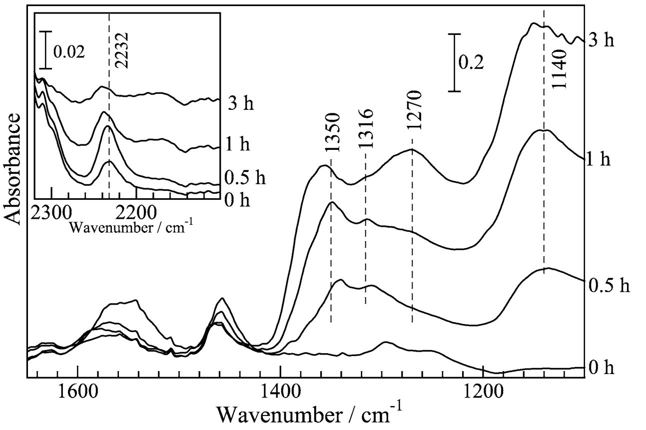

Fig. 6. Effect of 50 ppm SO_2 addition on the IR spectra of adsorbed species on 4 wt% Ag/Al_2O_3 during H_2–C_3H_8-SCR with 3% H_2O at 623 K. Before the measurement the catalyst was exposed to a flow of $H_2O/O_2/H_2/NO/C_3H_8$ for 2 h at 623 K. Conditions are the same as in Fig. 2 except for SV (SV $=$ 95,000 h^{-1}).

1350, 1316, 1270, 1200, and 1140 cm^{-1} are observed in the spectra. It is well known that SO_2 is oxidized by O_2 over alumina [25] and transition metal on alumina [26] to form adsorbed sulfates, and thus the above bands can be assigned to sulfate species adsorbed on different sites. According to the previous IR studies on the sulfates formation over alumina, bands in the range 1340–1380 cm^{-1} are assigned to sulfates on alumina (Al–$SO_4{}^{2-}$) [25,26]. As the reaction temperature increases, the intensity of the bands assigned to Al–$SO_4{}^{2-}$ (1366 and 1350 cm^{-1}) increases and, in contrast, the intensity of the bands at 1316, 1270, 1200 and 1140 cm^{-1} decreases (Fig. 4B). The thermal stability of surface species was evaluated by purging in He at 423 K (spectrum g). The intensity of the bands at 1316, 1270, 1200, and 1140 cm^{-1} was decreased by purging in He, whereas the bands assigned to Al–$SO_4{}^{2-}$ (1366 and 1350 cm^{-1}) increased. These results indicate that sulfate species related to the bands at 1316, 1270, 1200, and 1140 cm^{-1} are thermally less stable than Al–$SO_4{}^{2-}$ (at 1366 and 1350 cm^{-1}). Waquif et al. [26], in a detailed IR study on sulfate formation by $SO_2 + O_2$ reaction over CuO, copper/alumina, and alumina, assigned the IR bands at 1220–1080, 1290, and 1370 cm^{-1} to bulk-like $CuSO_4$, surface sulfate linked to Cu^{2+} and Al^{3+} ions (SO_3 groups linked to surface Cu–O and Al–O pair sites), and surface sulfate linked to Al^{3+} ions, respectively. Their results demonstrated the lower thermal stability of the sulfate on Cu–O and Al–O pair sites (1280–1180 cm^{-1} region) compared with the sulfate on Al–O site (1370 cm^{-1}). Meunier and Ross [14] studied SO_2 adsorption on Ag/Al_2O_3 and tentatively assigned the IR band at 1315 cm^{-1} to sulfate species linked to solely or partly to the silver phase. Taking into account our IR result that the sulfate species exhibiting bands at 1316, 1270, 1200, and 1140 cm^{-1} are thermally less stable than Al–$SO_4{}^{2-}$ (at 1366 and 1350 cm^{-1}), we can conclude that the bands at 1316, 1270, 1200, and 1140 cm^{-1} are assigned to sulfates on silver-containing sites.

Fig. 4A also shows IR spectra of adsorbed species on 4 wt% Ag/Al_2O_3 during C_3H_8-SCR in the presence of SO_2 and H_2O (spectrum e) or during H_2–C_3H_8-SCR in the presence of SO_2 and H_2O (spectrum f) at 773 K. The features of these spectra in a range of 1400–1100 cm^{-1} are close to that for the $SO_2/H_2O/O_2/H_2$ reaction at 773 K (spectrum d). Note that the bands at 1460 and 1550 cm^{-1} are assigned to the acetate [9,20]. These results indicate that the structure and coverage of the sulfates on Ag/Al_2O_3 do not markedly depend on the presence of hydrogen, NO, and C_3H_8. IR spectra of adsorbed species on Ag/Al_2O_3 during H_2–C_3H_8-SCR in the presence of SO_2 and H_2O at 773 K as a function of silver loading are shown in Fig. 5. Over alumina (Ag $=$ 0 wt%), bands centered at 1360 cm^{-1} assigned to sulfates on alumina (Al–$SO_4{}^{2-}$) are observed. In contrast, in the spectra for high-loading Ag/Al_2O_3 samples, the intensity of the bands at 1316 and 1270 cm^{-1} with respect to that of the Al–$SO_4{}^{2-}$ bands (at 1350–1360 cm^{-1}) is relatively high. This result supports the IR band assignment mentioned above; the broad bands centered around 1316 and 1270 cm^{-1} are assigned to sulfates on silver sites (Ag–$SO_4{}^{2-}$).

Changes in the IR spectra of adsorbed species on 4 wt% Ag/Al_2O_3 during H_2–C_3H_8-SCR are shown in Fig. 6 as a function of SO_2 cofeeding time. Note that the contact time for this experiment is 5 times lower than that for the catalytic test in Fig. 3. Before SO_2 cofeeding, bands assignable to acetate (1460 cm^{-1}), nitrates (1220–1300 cm^{-1}) [9,20], and NCO species on an Ag site designated Ag–NCO (2232 cm^{-1}) [27] were observed. When SO_2 was added to the mixture for 0.5 h, bands assignable to Al–$SO_4{}^{2-}$ (at around 1340–1366 cm^{-1}) and Ag–$SO_4{}^{2-}$ (at 1270 and 1316 cm^{-1}) appeared, and the intensity of Ag–NCO band (at 2232 cm^{-1}) increased. As SO_2 cofeeding time increased, the intensity of sulfates bands significantly increased and that of the Ag–NCO band deceased.

From these results, the temporal increase in NO conversion after SO_2 cofeeding at 623 K (Fig. 3) may be explained as follows. On SO_2 addition, sulfates of low surface coverage initially enhances NO reduction by promoting NCO formation, but further increases in sulfate coverage decrease the number of the active site available for the formation and adsorption of NCO intermediate. Note that the enhanced NO conversion

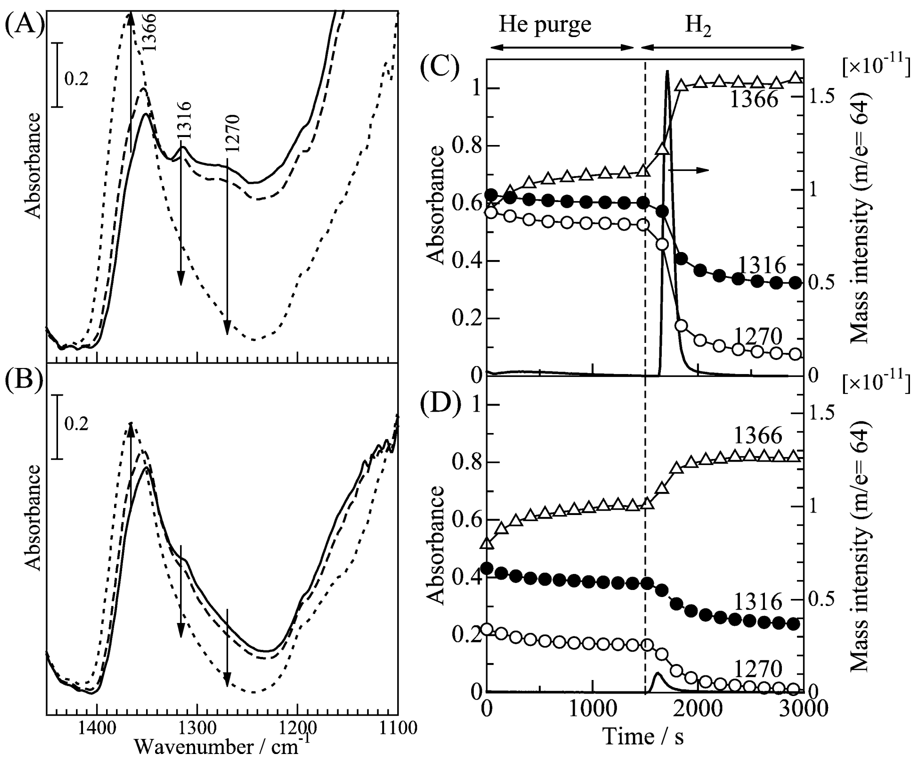

Fig. 7. Changes in the IR spectra of adsorbed species on Ag/Al_2O_3 with silver loading of (A) 4 wt% and (B) 2 wt% (623 K). Spectra were taken after flowing $SO_2/H_2O/O_2/H_2/NO/C_3H_8$ for 120 min (—) followed by He purge for 25 min (- - -), and by switching to flowing H_2 for 20 min (···). (C, D) The time course of IR band intensities for $Al–SO_4^{2-}$ (1366 cm^{-1}) and $Ag–SO_4^{2-}$ (1315, 1270 cm^{-1}) over of (C) 4 wt% and (D) 2 wt% catalysts. Solid lines in C and D denote MS intensity of SO_2 ($m/e = 64$) observed by on-line mass spectroscopy.

and increased IR intensity of the Ag–NCO band were reported by Park and Boyer [17] for C_3H_6-SCR reaction over 5 wt% Ag/Al_2O_3. These authors proposed that the silver sulfate is responsible for these phenomena. In our previous study on the mechanism of HC-SCR over Ag/Al_2O_3, we proposed that the reaction of nitrates with partially oxidized hydrocarbon species to produce NCO species is a crucial step in the HC-SCR reaction [10]. Bion et al. [28] proposed that NCO formation over Ag/Al_2O_3 occurs via nitration of hydrocarbons. It is well known that liquid-phase nitration of hydrocarbons is promoted by the presence of acids such as concentrated H_2SO_4. Thus, it is reasonable to assume that NCO formation via nitration of hydrocarbon derivatives is promoted by surface sulfates on Ag/Al_2O_3.

3.3. Reduction and desorption of sulfate

The reactivity of the each sulfate species ($Ag–SO_4^{2-}$ and $Al–SO_4^{2-}$) toward hydrogen was examined by the transient response of the IR spectra at 623 K (Fig. 7). The Ag/Al_2O_3 samples with different silver loading (2 and 4 wt%) were first exposed to the H_2–C_3H_8-SCR reaction mixture in the presence of SO_2 and H_2O for 2 h to produce sulfates on the catalyst surface. The intensities of the bands due to $Ag–SO_4^{2-}$ species (1316 and 1270 cm^{-1}) are higher for the 4 wt% catalyst (Fig. 7A) than for the 2 wt% catalyst (Fig. 7B). These bands decreased slightly after purging with He for 25 min, and the intensities of the bands due to $Al–SO_4^{2-}$ (at around 1350–1366 cm^{-1}) simultaneously increased slightly. When the flowing gas was switched to 0.5% H_2, the intensities of the bands due to $Ag–SO_4^{2-}$ decreased, whereas the intensity of the band due to $Al–SO_4^{2-}$ increased. The effect of silver loading on the relative rates of decrease for $Ag–SO_4^{2-}$ adspecies during the reaction with hydrogen can be evaluated by comparing the slopes of the curves in Figs. 7C and 7D. Clearly, the rate of decrease in $Ag–SO_4^{2-}$ bands (at 1316 and 1270 cm^{-1}) is higher for the high loading sample (4 wt%). Mass spectroscopy directly connected to the in situ IR flow cell was used to provide information on the gas-phase products in the reaction of adsorbed sulfates with hydrogen; the results are shown in Figs. 7C and 7D. When the pretreated catalyst was exposed to hydrogen, SO_2 ($m/e = 64$) was produced, and the amount of desorbed SO_2 estimated from integrated area of the SO_2 desorption peak was $>$ 10 times larger for the 4 wt% sample (0.042 mmol g^{-1}) than for 2 wt% sample (0.0038 mmol g^{-1}). Note that H_2S ($m/e = 34$) was not observed by mass spectroscopy. These results indicate that the sulfates adsorbed on silver site were reduced by hydrogen to gas-phase SO_2, and that more SO_2 is desorbed for the higher silver loading sample. They also demonstrate that sulfate on silver-containing sites ($Ag–SO_4^{2-}$) is converted to gas-phase SO_2 or migrates to the alumina surface-forming sulfate on Al sites.

SO_2 desorption profiles during TPD/TPR experiments for the sulfated 4 wt% Ag/Al_2O_3 in a flow of He (curve b) and in a flow of 0.5% H_2 in He (curve a) are shown in Fig. 8. Before the measurements, samples were pretreated in flowing

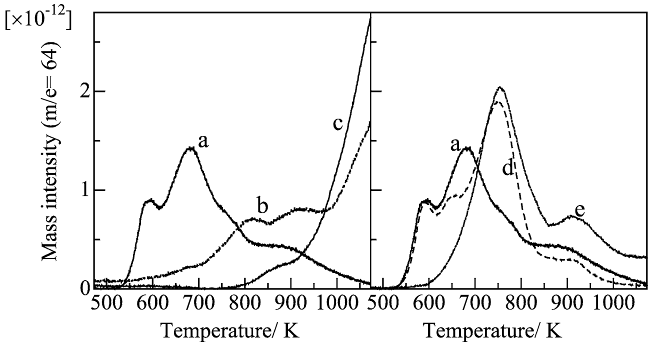

Fig. 8. SO_2-TPD/TPR curves ($m/e = 64$) for 4 wt% Ag/Al_2O_3 in flowing 0.5% H_2, (b) 4 wt% Ag/Al_2O_3 in flowing He, (c) 2 wt% Ag/Al_2O_3 in flowing He, (d) 3 wt% Ag/Al_2O_3 in flowing 0.5% H_2, and (e) 2 wt% Ag/Al_2O_3 in flowing 0.5% H_2. Samples were pre-treated in flowing $SO_2/H_2O/O_2/H_2/NO/C_3H_8$ for 7 h at 623 K.

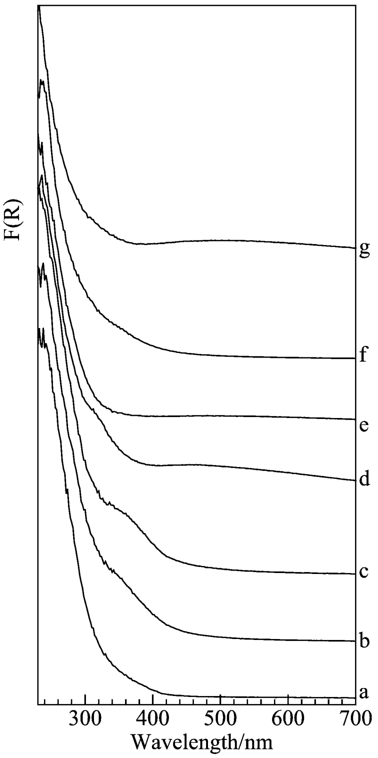

Fig. 9. UV–vis spectra of (a–e) 4 wt% Ag/Al_2O_3 and (f, g) 2 wt% Ag/Al_2O_3 after the pre-treatment in various gas mixtures at 623 K: (a) in $O_2/NO/C_3H_8$ for 0.5 h, (b) in O_2/H_2 for 0.5 h, (c) in $O_2/H_2/NO/C_3H_8$ for 0.5 h, (d) in $SO_2/H_2O/O_2/H_2/NO/C_3H_8$ for 7 h, (e) in $SO_2/H_2O/O_2/NO/C_3H_8$ for 7 h (f) in $O_2/H_2/NO/C_3H_8$ for 0.5 h, and (g) in $SO_2/H_2O/O_2/H_2/NO/C_3H_8$ for 7 h.

$SO_2/H_2O/O_2/H_2/NO/C_3H_8$ for 7 h at 623 K. SO_2 desorption in the presence of hydrogen occurs at lower temperature than in the thermal desorption condition, indicating that hydrogen promotes the removal of sulfates from the catalyst surface. The effect of silver loading on the thermal stability and reducibility of the sulfate species was evaluated by comparing the TPD/TPR profiles of different silver loading catalysts pretreated in flowing $SO_2/H_2O/O_2/H_2/NO/C_3H_8$ for 7 h at 623 K. SO_2 desorption occurs at lower temperature for the higher loading sample in thermal desorption conditions (curves b and c) as well as in hydrogen reduction conditions (curves a, d, and e). The amount of SO_2 desorbed during the TPR experiments in the range of 473–1073 K was calculated; the value for the 2 wt% sample (curve e, 0.45 $mmol\,g^{-1}$, $S/Ag = 2.4$) was higher than that for the 4 wt% sample (curve a, 0.37 $mmol\,g^{-1}$, $S/Ag = 1.0$). This indicates that more sulfates formed on the surface during H_2–C_3H_8-SCR in the presence of SO_2 and H_2O for the low silver loading catalyst.

3.4. *Effect of SO_2 on the structure of Ag species*

To evaluate the effect of SO_2 and hydrogen on the structure of silver species over silver alumina under the reaction condition, UV–vis spectrum of silver alumina samples after various pretreatments are shown in Fig. 9. The sample was exposed to various gas mixtures at 623 K and quenched at room temperature. Then UV–vis spectra of the quenched sample were measured at room temperature after the sample was transferred to an optical quartz cell without being exposed to air. The spectrum taken after the C_3H_8-SCR reaction with the 4 wt% sample (spectrum a) exhibits a band assignable to the $4d^{10}$ to $4d^9s^1$ transition of the Ag^+ ion (<240 nm) [29] and no band due to metallic Ag species at a higher-wavelength region. The spectrum is almost identical to that obtained after the oxidation in 10% O_2 at 773 K (not shown). This indicates that Ag^+ ions are the predominant Ag species before the reaction and under the C_3H_8-SCR reaction condition at 623 K. In the spectrum obtained after H_2–C_3H_8-SCR reaction (spectrum c), as well as that after the exposure of H_2/O_2 mixture (spectrum b), a band due to Ag^+ ions (<240 nm) and a broad shoulder band at around 300–400 nm are observed. We previously reported that the latter bands were observed on silver alumina catalyst by in situ UV–vis during H_2/O_2 reaction at 523 K [21]. Sazama et al. [24] observed a band at around 250–330 nm by in situ UV–vis during a H_2-decane-SCR reaction and assigned it to the $4d^{10}5s^1 \to 4d^95s^15p^1$ and $4d^{10}5s^1 \to 4d^95s^16p^1$ transitions in ${Ag_n}^{\delta+}$ cluster with $n \leqslant 8$ [29]. Thus, spectrum c in Fig. 9 indicates that Ag^+ ion and ${Ag_n}^{\delta+}$ cluster coexist during the H_2–C_3H_8-SCR reaction.

After the measurements of the spectrum during H_2–C_3H_8-SCR, SO_2/H_2O gas mixture was added to the reaction mixture, and the catalyst was exposed to the gas mixture at 623 K for 7 h. Then the UV–vis spectrum was taken (spectrum d). The band assignable to an ${Ag_n}^{\delta+}$ cluster at around 300–340 nm was observed, although it was of higher energy than that for the nondeactivated sample (spectrum c). In addition, a band due to Ag^+ ions (at <240 nm) and a broad band at around 400–700 nm assignable to large Ag metal particles [29] were observed, indicating that Ag^+ ions, the ${Ag_n}^{\delta+}$ cluster, and large Ag metal particles coexist in the sample. In contrast, the spectrum of the deactivated 2 wt% Ag/Al_2O_3 sample obtained under the same conditions (spectrum g) shows a band due to Ag^+ ions (at <240 nm) and a band due to the large Ag metal particles (at 400–700 nm), but the intensity of the band due to ${Ag_n}^{\delta+}$ cluster was significantly lower than that for the 4 wt% Ag/Al_2O_3 sample. In the UV–vis spectrum of the 4 wt% Ag/Al_2O_3 sample during C_3H_8-SCR with the SO_2/H_2O mixture (in the absence of hydrogen), the band due to Ag^+ ions (at <240 nm) was predominant, but no band due to $Ag_n^{\delta+}$ cluster was observed (spectrum e). Summarizing UV–vis results, a fraction of Ag^+ species were reduced by hydrogen to partially reduced $Ag_n^{\delta+}$ clusters during H_2–C_3H_8-SCR even in the presence of SO_2, and the amount of $Ag_n^{\delta+}$ clusters was larger on the higher-loading sample (4 wt%).

3.5. Possible reasons for improved SO_2 tolerance

From the above experiments, the effect of hydrogen addition on SO_2 tolerance of Ag/Al_2O_3 can be summarized as follows. In the absence of hydrogen, NO and C_3H_8 conversions are decreased by adding 50 ppm SO_2 because of the site blocking by strongly adsorbed sulfates on Ag/Al_2O_3. In the presence of hydrogen, the sulfates on silver-containing sites ($Ag–SO_4^{2-}$) are reduced and desorb as SO_2 or migrate to alumina surface-forming sulfates on Al sites ($Al–SO_4^{2-}$), which are relatively stable even in the presence of hydrogen at 623 K (Fig. 7). The TPR results shown in Fig. 8 also demonstrate that hydrogen promotes the removal of sulfates from the catalyst surface. UV–vis results (Fig. 9) shows that a fraction of the Ag^+ ions are reduced by hydrogen to partially reduced $Ag_n^{\delta+}$ clusters during H_2–C_3H_8-SCR even in the presence of SO_2, whereas Ag^+ ions are predominant in the absence of hydrogen. It is reasonable to assume that sulfate anions adjacent to the partially reduced silver sites are less stable than those on cationic sites. Therefore, we propose that the improved SO_2 tolerance of Ag/Al_2O_3 catalyst by hydrogen addition is caused by the reduction of sulfates to SO_2 over silver sites and its subsequent desorption, and that these steps should be more advantageous over partially reduced $Ag_n^{\delta+}$ cluster sites than over Ag^+ sites.

The SO_2 tolerance of Ag/Al_2O_3 in H_2–C_3H_8-SCR depends strongly on the silver loading. Although the activity in the absence of SO_2 is higher for the lower silver loading catalyst, the highest activity in the presence of SO_2 is achieved on the medium-loading sample (3 wt%), and the SO_2 tolerance factor is highest for the 4 wt% Ag/Al_2O_3 (Fig. 2). The relative intensity of the $Ag–SO_4^{2-}$ band (at 1270 cm^{-1}) compared with the $Al–SO_4^{2-}$ band (at 1350 cm^{-1}) is also highest at silver loading of 4 wt% (Fig. 2). TPD/TPR results show that the thermal decomposition and reduction of sulfates occurs at lower temperatures for the higher-loading sample and that the number of sulfates adspecies formed during H_2–C_3H_8-SCR in the coexistence of SO_2 is lower for the higher-loading sample. UV–vis result shows that the amount of partially reduced $Ag_n^{\delta+}$ clusters during H_2–C_3H_8-SCR in the presence of SO_2 is larger for the higher-loading sample. Therefore, we propose that the higher SO_2 tolerance of high-loading catalyst for the H_2–C_3H_8-SCR reaction is caused by the higher rate of sulfate reduction, which is more advantageous over partially reduced silver sites than over Ag^+ sites. In the literature on HC-SCR with Ag/Al_2O_3, several authors have shown that silver loading >2 wt% demonstrated optimal lean-NO_x performance in the presence of SO_2. Abe et al. [15] and Sumiya et al. [13] reported that 4–5 wt% Ag/Al_2O_3 showed moderate SO_2 resistance for EtOH-SCR. Angelidis et al. [16] and Park et al. [17] reported that SO_2 resistance of silver alumina catalyst for C_3H_6-SCR was dependent on the silver loading, and that 5 wt% Ag/Al_2O_3 showed high SO_2 resistance. Considering our results, the higher SO_2 resistance of 4–5 wt% Ag/Al_2O_3 catalysts for HC-SCR reported in the literature could also be ascribed to the facile sulfates decomposition over high silver loading catalysts.

4. Conclusion

SO_2 tolerance of Ag/Al_2O_3 for C_3H_8-SCR is improved by H_2 cofeeding and increased Ag loading. Sulfates strongly adsorbed on silver-containing sites are removed form the catalyst surface by a flow of H_2-containing mixtures, resulting in the formation of gas-phase SO_2 or sulfates on alumina. A fraction of Ag^+ ions are reduced by hydrogen to partially reduced $Ag_n^{\delta+}$ clusters during H_2–C_3H_8-SCR even in the presence of SO_2, whereas Ag^+ ions are predominant in the absence of hydrogen. The thermal decomposition and H_2 reduction of sulfates occurs at lower temperature for the higher-loading sample, and the amount of partially reduced $Ag_n^{\delta+}$ clusters during H_2–C_3H_8-SCR in the presence of SO_2 is larger for the higher-loading sample. Therefore, improved SO_2 tolerance of Ag/Al_2O_3 by H_2 cofeeding and increased Ag loading can be explained by the reductive promotion of sulfate removal possibly accelerated by the partially reduced silver site.

Acknowledgments

This work was partly supported by a grant-in-aid from the Japanese Ministry of Education, Science and Culture and by a feasibility study sponsored by the Japanese Science and Technology Agency.

References

[1] M. Iwamoto, Catal. Today 29 (1996) 29.
[2] H. Hamada, Catal. Today 22 (1994) 21.
[3] R. Burch, J.P. Breen, F.C. Meunier, Appl. Catal. B 39 (2002) 283.
[4] R. Burch, Catal. Rev. 46 (2004) 271.
[5] T. Miyadera, K. Yoshida, Chem. Lett. (1993) 1483.
[6] T. Miyadera, Appl. Catal. B 2 (1993) 199.
[7] N. Aoyamoa, K. Yoshida, A. Abe, T. Miyadera, Catal. Lett. 43 (1997) 249.
[8] T. Nakatsuji, R. Yasukawa, K. Tabata, K. Ueda, M. Niwa, Appl. Catal. B 17 (1998) 333.
[9] K. Shimizu, A. Satsuma, T. Hattori, Appl. Catal. B 25 (2000) 239.
[10] K. Shimizu, J. Shibata, H. Yoshida, A. Satsuma, T. Hattori, Appl. Catal. B 30 (2001) 151.
[11] L.-E. Lindfors, K. Eranen, F. Klingstedt, D.Yu. Murzin, Top. Catal. 28 (2004) 185.
[12] S. Satokawa, K. Yamaseki, H. Uchida, Appl. Catal. B 34 (2001) 299.
[13] S. Sumiya, M. Saito, H. He, Q.C. Feng, N. Takezawa, K. Yoshida, Catal. Lett. 50 (1998) 87.
[14] F.C. Meunier, J.R.H. Ross, Appl. Catal. B 24 (2000) 23.
[15] A. Abe, N. Aoyama, S. Sumiya, N. Kakuta, K. Yoshida, Catal. Lett. 51 (1998) 5.
[16] T.N. Angelidis, S. Christoforou, A. Bongiovanni, N. Kruse, Appl. Catal. B 39 (2002) 197.
[17] P.W. Park, C.L. Boyer, Appl. Catal. B 59 (2005) 27.
[18] S. Satokawa, Chem. Lett. (2000) 294.
[19] S. Satokawa, J. Shibata, K. Shimizu, A. Satsuma, T. Hattori, Appl. Catal. B 42 (2003) 179.
[20] J. Shibata, K. Shimizu, S. Satokawa, A. Satsuma, T. Hattori, Phys. Chem. Chem. Phys. 5 (2003) 2154.

[21] A. Satsuma, J. Shibata, A. Wada, Y. Shinozaki, T. Hattori, Stud. Surf. Sci. Catal. 145 (2002) 235.

[22] M. Richter, U. Bentrup, E. Eckelt, M. Schneider, M.-M. Pohl, R. Fricke, Appl. Catal. B 51 (2004) 261.

[23] R. Burch, J.P. Breen, C.J. Hill, B. Krutzsch, K. Konrad, E. Jobson, L. Cider, K. Eränen, F. Klingstedt, L.-E. Lindfors, Top. Catal. 30/31 (2004) 19.

[24] P. Sazama, L. Capek, H. Drobna, Z. Sobalik, J. Dedecek, K. Arve, B. Wichterlova, J. Catal. 232 (2005) 344.

[25] M.B. Mitchell, V.N. Sheinker, M.G. White, J. Phys. Chem. 100 (1996) 7550.

[26] W. Waquif, O. Saur, J.C. Lavalley, S. Perathoner, G. Centi, J. Phys. Chem. 95 (1991) 4501.

[27] S. Kameoka, T. Chafik, Y. Ukisu, T. Miyadera, Catal. Lett. 55 (1998) 211.

[28] N. Bion, J. Saussey, M. Haneda, M. Daturi, J. Catal. 217 (2003) 47.

[29] A.N. Pestryakov, A.A. Davydov, J. Electron Spectrosc. Relat. Phenom. 74 (1995) 195.